Eur. Phys. J. C 31, 57–71 (2003)
Digital Object Identifier (DOI) 10.1140/epjc/s2003-01315-1

THE EUROPEAN PHYSICAL JOURNAL C

QCD explanation of oscillating hadron and jet multiplicity moments

M.A. Buican, C. Förster, W. Ochs

Max-Planck-Institut für Physik (Werner-Heisenberg-Institut), Föhringer Ring 6, 80805 München, Germany

Received: 21 July 2003 /
Published online: 26 September 2003 –

Abstract. Ratios of multiplicity moments, H_q (cumulant over factorial moments K_q/F_q), have been observed to show an oscillatory behavior with respect to order, q. Recent studies of e^+e^- annihilations at LEP have shown, moreover, that the amplitude and oscillation length vary strongly with the jet resolution parameter $y_{\rm cut}$. We study the predictions of the perturbative QCD parton cascade assuming low non-perturbative cut-off ($Q_0 \sim \Lambda_{\rm QCD} \sim$ few 100 MeV) and derive the expectations as a function of the CMS energy and jet resolution from threshold to very high energies. We consider numerical solutions of the evolution equations of gluodynamics in double logarithmic and modified leading logarithmic approximations (DLA, MLLA), as well as results from a parton MC with readjusted parameters. The main characteristics are obtained in MLLA, while a more numerically accurate description is obtained by the MC model. A unified description of correlations between hadrons and correlations between jets emerges, in particular for the transition region of small $y_{\rm cut}$.

1 Introduction

The multiplicity of hadrons is the simplest global characteristic of the final state in particle collisions. It was an early conjecture that the main trends of the mean multiplicity and higher multiplicity moments could be reproduced by the corresponding perturbative QCD calculations for the quark–gluon cascade. First results have been derived for the asymptotic high energy limit in application of the double logarithmic approximation (DLA) [1–3]. Taking into account the leading contributions from the collinear and soft radiation singularities and angular ordering [4,5] one arrives at a probabilistic description of the parton cascade which evolves from the high energy scale Q down to the hadronization scale Q_0. The perturbative expansion in the coupling $\alpha_{\rm s}$ can be resummed and the exponent can be expanded into a power series of $\sqrt{\alpha_{\rm s}}$. In this way results on mean multiplicity [5,3,6] and higher moments [2,3,7] have been obtained, subsequently the next-to-leading log corrections in MLLA [8–11] and yet higher order terms [12–14] have been derived. All these results can be obtained as different approximations to the MLLA evolution equations for the generating function of quark and gluon jets [15]. A full solution of these equations can be obtained by numerical methods [16,17].

One motivation of such studies was – and still is – to find out how far one can extend perturbative calculations into the regime of real strong interactions which determine multiparticle production. In this way, we hope to learn more about the color confinement mechanism. The MLLA results on mean multiplicities and single particle spectra give a surprisingly good description of the data which led to the notion of "local parton hadron duality" (LPHD [9]). The results here depend on only two parameters, the QCD scale Λ and a single non-perturbative parameter, the transverse momentum cut-off Q_0 with $Q_0 \gtrsim \Lambda$; an overall normalization factor K is also allowed for. Such parton level calculations have been applied to a large variety of inclusive observables, in particular to multiparticle correlations ("generalized LPHD" [18]); even quasi-exclusive processes are within reach [19]. In general, one observes that with increasing accuracy, the perturbatively calculated observables are in better agreement with the data. This simple model does not contain any hadronic resonances, so it is clear that it can only describe sufficiently inclusive observables and should not be considered for too restricted regions of phase space (for pertinent reviews, see [20–23]).

Whereas there is no problem with inclusive single particle results, the status of higher multiplicity moments (factorial moments F_q and cumulant moments K_q, see below), which are integrals over the respective q particle correlation functions, is more controversial. The data on quark and gluon jets for $q \leq 5$ [24] deviate with increasing order q from the higher order logarithmic approximations [25]; they correspond to an expansion in $q\sqrt{\alpha_{\rm s}}$ rather than $\sqrt{\alpha_{\rm s}}$ [20,22] and the known terms fit the mean multiplicity (moment $q = 1$) but the moments of higher order become much larger than the data. On the other hand, numerical solutions of the MLLA evolution equation yield very good agreement with these data [16,17]; remarkably, a common fit of hadron and jet multiplicities is possible and results in

$$K_{\rm tot} \approx 1 \tag{1}$$

for a small cut-off $Q_0 \gtrsim \Lambda$ where $K_{\rm tot}$ is the ratio of the total hadron to parton multiplicities. This ratio $K_{\rm tot} \approx 1$

was also found to be consistent with the quark and gluon multiplicities in high $p_{\rm T}$ jets observed at the TEVATRON [26] where the higher order MLLA corrections are taken into account as well.

An interesting prediction [13] from the asymptotic $\sqrt{\alpha_{\rm s}}$ expansion concerns the ratio of moments

$$H_q = K_q/F_q. \tag{2}$$

These moments show an oscillatory behavior with the first minimum at

$$q_{\min} \approx \frac{1}{h_1\gamma_0}+\frac{1}{2}+\mathcal{O}(\gamma_0), \quad h_1=\frac{11}{24}, \quad \gamma_0^2=\frac{2N_C\alpha_{\rm s}}{\pi}, \tag{3}$$

where $N_C = 3$ and γ_0 denotes the leading order multiplicity anomalous dimension at the considered energy scale, numerically $q_{\min} \approx 5(\pm 1)$ at LEP energies. Such oscillations have indeed been observed in e^+e^- annihilations at SLC [27] and recently at LEP [28,29] with the first minimum at $q_{\min} \approx 5$ as expected.

Since the absolute size of the moments are not in quantitative agreement with these high energy predictions the physical origin of these oscillations remains controversial. It has been noted that the truncation of the multiplicity distribution at large multiplicity, n, also gives rise to oscillations [30]. Furthermore, a superposition of two components (like 2 and 3 jet events), each one modeled without oscillations, can lead to oscillations in the full sample [31].

A new element has been brought into the discussion recently through analyses of the L3 measurements [28,29] of multiplicity moments for hadrons and narrow jets at high resolution (small $y_{\rm cut}$ parameter). The measurements feature a rapid variation of both the oscillation amplitude and oscillation length in q as function of $y_{\rm cut}$. This behavior does not appear in the asymptotic solutions of the evolution equation [13].

In this paper we aim at an understanding, within perturbative QCD, of the H_q oscillation phenomena in both hadron and jet final states. We study first the solutions of the evolution equations (both DLA and MLLA) with jet hardness from threshold up to the asymptotic regime; furthermore, we investigate the variations of the jet multiplicity moments with resolution, from low resolution (fat jets) up to high resolution (narrow jets) – ultimately up to the scale for the parton–hadron transition. These calculations depend only on the QCD scale, Λ, and on one parameter, $Q_{\rm c}$, which refers to the transverse momentum cut-off. This transverse momentum cut-off is given by either the scale of the arbitrarily chosen jet resolution or the characteristic hadronic scale $Q_{\rm c} = Q_0$. The full results including the dependence on $Q_{\rm c}$, are obtained by numerical methods. The need for an overall normalization factor K is considered for the mean multiplicity.

A similar theoretical scheme is realized in a parton level MC (ARIADNE [32]) which is based on sequential parton radiation from color dipoles [33,34] with a $k_{\rm T}$ cut-off. We have readjusted the parameters Λ and Q_0 in this MC to describe hadronic final states without an additional hadronization phase, assuming again a duality between hadron and parton final states at scale Q_0.

2 Definition of moments and jet resolution

The distribution, P_n, of the multiplicity, n, of particles or jets in an event can be characterized by its moments. One considers the factorial moments f_q or the normalized moments F_q

$$\begin{aligned} f_q &= \sum_{n=0}^{\infty} n(n-1)\dots(n-q+1)P_n, \\ F_q &= f_q/N^q, \qquad N \equiv f_1, \end{aligned} \tag{4}$$

with mean multiplicity N. Furthermore, one introduces the cumulant moments k_q and K_q which are used to measure the genuine correlations without uncorrelated background in a multiparticle sample

$$k_q = f_q - \sum_{i=1}^{q-1} \binom{q-1}{i} k_{q-i} f_i, \qquad K_q = k_q/N^q, \tag{5}$$

in particular $K_2 = F_2 - 1,\ K_3 = F_3 - 3F_2 + 2$; for a Poisson distribution $K_1 = 1,\ K_q = 0$ for $q > 1$.

These moments can also be obtained from the generating function of the multiplicity distribution

$$Z(Y,u) = \sum_{k=0}^{\infty} P_n(Y)\ u^k \tag{6}$$

by differentiation

$$f_q = \frac{{\rm d}^q}{{\rm d}u^q} Z(Y,u)\Big|_{u=1}, \qquad k_q = \frac{{\rm d}^q}{{\rm d}u^q} \ln Z(Y,u)\Big|_{u=1}, \tag{7}$$

where Y denotes here some kinematic variable like the total energy.

In a high energy collision, many hadrons are produced and they are found to cluster typically into jets of particles. The number of such jets depends on the resolution, which is defined through an algorithm in terms of a resolution parameter. In this paper, we choose the so-called Durham algorithm [35]. At resolution $y_{\rm cut}$ one combines particles into jets iteratively until all pairs of jets or particles have relative transverse momentum $k_{\rm T}^2 > y_{\rm cut}Q^2$ for small relative angles Θ_{ij}, or, in general,

$$y_{ij} = 2\min\left(E_i^2, E_j^2\right)(1-\cos\Theta_{ij})/Q^2 > y_{\rm cut}. \tag{8}$$

In our application to e^+e^- annihilation, Q is the total CMS energy. At very low resolution ($y_{\rm cut} \to 1$) one sees only two jets which evolve from the primary $q\overline{q}$ system, whereas with increasing resolution more and more jets are resolved until at very high resolution ($y_{\rm cut} \to 0$) all final state hadrons are resolved, so

$$\begin{aligned} y_{\rm cut} &\to 1: \ N_{\rm jet} = 2, \\ y_{\rm cut} &\to 0: \ N_{\rm jet} = N_{\rm hadron}. \end{aligned} \tag{9}$$

In this paper we study both the multiplicity of jets and the multiplicity of hadrons and the respective moments.

In particular, we are interested in the variation of these observables with energy and resolution as has recently been reported in the experimental works [28,29].

In the popular Monte Carlo models of today, the parton cascade is terminated at a scale of $Q_0 \sim 1\,\mathrm{GeV}$; this perturbative phase is followed by the hadronization phase for which non-perturbative models, typically with a rather large number of parameters, are introduced. In our calculation we follow the idea of LPHD [9] and let the parton cascade evolve further down to a lower scale Q_0 of a few 100 MeV of the order of the QCD scale Λ itself. Then we compare the result directly to the hadron final state. In this way, besides the common parameter Λ only one extra non-perturbative parameter Q_0 is introduced which can be interpreted either as a typical hadron mass or as inverse hadron radius. In the theoretical calculations we obtain the hadronic final state for $Q_\mathrm{c} \to Q_0$ and we replace (9) by

$$\begin{aligned} y_\mathrm{cut} \to 1 &: \; N_\mathrm{jet} = 2, \\ y_\mathrm{cut} \to (Q_0/Q)^2 &: \; N_\mathrm{jet} = N_\mathrm{hadron}. \end{aligned} \tag{10}$$

An important feature is the transition from jets to hadrons for small resolution parameter y_cut which tests the hadronization models in the region of small momentum transfers, the so-called "soft" region. In this paper the consequences of such an approach for multiparticle correlations in the soft region is investigated in the theoretical models and compared with the data.

3 Solution of evolution equations for multiplicity moments

3.1 Double logarithmic approximation

In this approximation we consider a single jet of particles or sub-jets at transverse momentum cut-off $k_\mathrm{T} > Q_\mathrm{c}$; for e^+e^- annihilation, two jets have to be superimposed, with Q_c then corresponding to the resolution y_cut. Only the most singular terms of the parton splitting functions are kept and recoil effects are neglected. Then we can restrict ourselves to gluodynamics, i.e. we neglect the production of quark–anti-quark pairs which would represent a non-leading contribution. A common simplification of these calculation is the restriction to 1-loop results; furthermore, in this application we consider only light quarks. In this case, the generating function follows an evolution equation [3,7,36]:

$$\frac{\mathrm{d}Z(Y_\mathrm{c},u)}{\mathrm{d}Y_\mathrm{c}} = Z(Y_\mathrm{c},u) \int_0^{Y_\mathrm{c}} \mathrm{d}y' \gamma_0^2(y')[Z(y',u)-1], \tag{11}$$

$$Z(0,u) = u, \tag{12}$$

with the multiplicity anomalous dimension

$$\gamma_0^2(y) = \frac{2N_C\alpha_\mathrm{s}(y)}{\pi} = \frac{\beta^2}{y+\lambda_c}, \tag{13}$$

$$Y_\mathrm{c} = \ln(E/Q_\mathrm{c}), \quad \lambda_c = \ln(Q_\mathrm{c}/\Lambda), \quad \beta^2 = \frac{4N_C}{b},$$
$$b = \frac{11}{3}N_C - \frac{2}{3}n_f, \tag{14}$$

where $N_c = 3$. The argument of α_s is related to the transverse momentum, i.e. $y = \ln(k_\mathrm{T}/Q_\mathrm{c})$. In our analytic calculations we take

$$\Lambda = 300\ \mathrm{MeV}, \quad \lambda = \ln(Q_0/\Lambda) = 0.015, \quad n_f = 3. \tag{15}$$

The initial condition (12) implies that at threshold ($Y_\mathrm{c} = 0$) the jet $Z(Y_\mathrm{c},u)$ contains only one particle (sub-jet).

Differentiating the evolution equation (11) with respect to u at $u = 1$, one obtains the following equation for the multiplicity, N:

$$N'(Y_\mathrm{c}) = \int_0^{Y_\mathrm{c}} \mathrm{d}y' \gamma_0^2(y') N(y'), \tag{16}$$

or, equivalently,

$$\begin{aligned} &N''(Y_\mathrm{c}) - \gamma_0^2(Y_\mathrm{c})N(Y_\mathrm{c}) = 0, \\ &N(0) = 1, \quad N'(0) = 0. \end{aligned} \tag{17}$$

This equation can be solved in terms of Bessel functions [3]:

$$\begin{aligned} N(Y_\mathrm{c}) = {} & 2\beta\sqrt{Y_\mathrm{c}+\lambda} \\ & \times \Big[I_1(2\beta\sqrt{Y_\mathrm{c}+\lambda}) K_0(2\beta\sqrt{\lambda}) \\ & + K_1(2\beta\sqrt{Y_\mathrm{c}+\lambda}) I_0(2\beta\sqrt{\lambda}) \Big]. \end{aligned} \tag{18}$$

This solution is shown in Fig. 1, for constant cut-off $Q_\mathrm{c} = Q_0$ as a full line, which represents the well-known increase of multiplicity, $N \sim \exp(2\beta\sqrt{E/\Lambda})$, and follows from the asymptotics of $I_\nu(z) \sim \mathrm{e}^z$.

One can also study the variation of jet multiplicity at fixed jet energy E with resolution Q_c, as discussed previously [16]. This dependence is given by the same function (18) if the Durham algorithm is applied; in this case the cut-off in the evolution of the parton cascade is defined through the transverse momentum $k_\mathrm{T} \geq Q_\mathrm{c}$. The corresponding result is represented by the dashed line in Fig. 1. One observes a considerably lower multiplicity by an order of magnitude, but, for decreasing $Q_\mathrm{c} \to Q_0$ ($Y_\mathrm{c} \to Y_0$) in the transition from jet $\to$ hadron, the jet curve rises rapidly and reaches the curve for hadrons. This behavior is a consequence of the running coupling, which is always smaller for jets, because k_T, the argument of α_s, is always larger. The analytic behavior in this limit can be derived from (18) using the approximation $K_0(z) \simeq \ln(2/z)$ for small z with small Q_c or large Y_c (see also [21])

$$N \sim (\beta^2 Y_\mathrm{c})^{1/4} \ln\left(\frac{1}{\beta\sqrt{\lambda_c}}\right) \exp 2\beta\sqrt{Y_\mathrm{c}}. \tag{19}$$

This multiplicity diverges logarithmically for $Q_\mathrm{c} \to \Lambda$ ($\lambda_c \to 0$). This divergence is a consequence of the diverging coupling in this limit. Since $Q_\mathrm{c} \geq Q_0 > \Lambda$, this

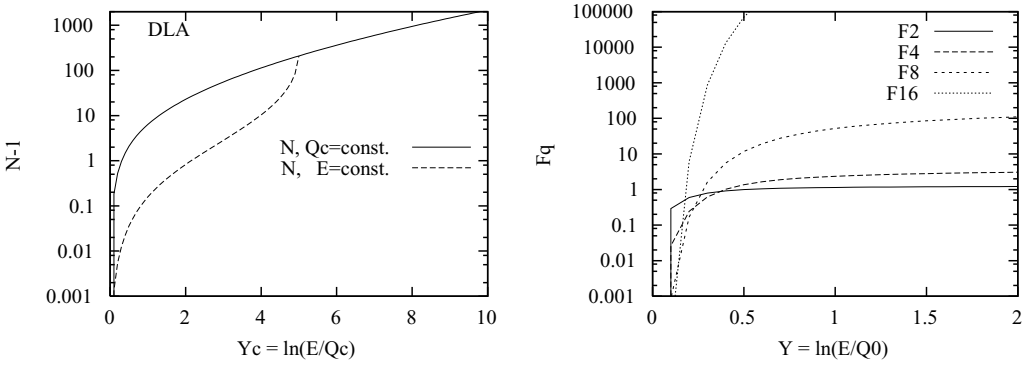

Fig. 1. Multiplicity, N, in DLA in a single jet versus jet energy E for fixed $Q_c = Q_0$ (representing hadrons) and for fixed energy E ($Y_0 = \ln(E/Q_0) = 5$) but variable resolution Q_c (or $y_{cut} = (Q_c/2E)^2$) (representing jets) and factorial moments F_q versus energy E (Y). The moments approach the asymptotic limits $F_2 = 1.33, F_4 = 4.62, F_8 = 359.7, F_{16} = 2 \times 10^8$

divergence is outside the physical region, but a strong variation remains, as seen in Fig. 1. Note that in the case of fixed coupling, the moments would only depend on the ratio E/Q_c as no other dimensional quantities exist; then both curves for jets and hadrons would coincide and follow asymptotically a power law $N \sim (E/Q_0)^{\gamma_0}$.

Next we calculate the factorial moments for $q > 1$. By appropriate differentiation of the evolution equation (11) one finds for $q > 1$:

$$f_q'(Y_c) = \int_0^{Y_c} \mathrm{d}y' \gamma_0^2(y') f_q(y') + \sum_{m=1}^{q-1} \binom{q}{n} f_m(y) \int_0^{Y_c} \mathrm{d}y' \gamma_0(y') f_{q-m}(y'), \tag{20}$$

$$f_q(0) = 0, \tag{21}$$

where (21) follows from (12) and (7), in agreement with (4).

This coupled system of integro-differential equations is solved numerically. The integral is computed using the trapezoidal rule with a step size of $\delta y = 10^{-5}$. As a test, we calculated the multiplicity from the analytic formula and compared with the numerical solution of (16). There was good agreement to within 10^{-4}. Reducing the step size by a factor of 10 ($\delta y = 10^{-6}$) resulted in a change of about 1% in the value of F_{16} and a change in the ratio H_5 by 0.1% below in the range considered.

A selection of results on the normalized moments F_q is also shown in Fig. 1. The moments F_q for $q > 1$ vanish at threshold $Y_c = 0$. Shortly above threshold the moments of higher rank q are suppressed as the multiplicity is low here and only a small number of terms contribute to the sum (4); on the other hand, they approach larger asymptotic values. In DLA one finds [2]

$$F_q = \frac{q}{q^2-1} \sum_{m=1}^{q-1} \binom{q}{m} \frac{F_m F_{q-m}}{m} \quad \text{for} \quad q > 1 \quad \text{with} \quad F_1 = 1, \tag{22}$$

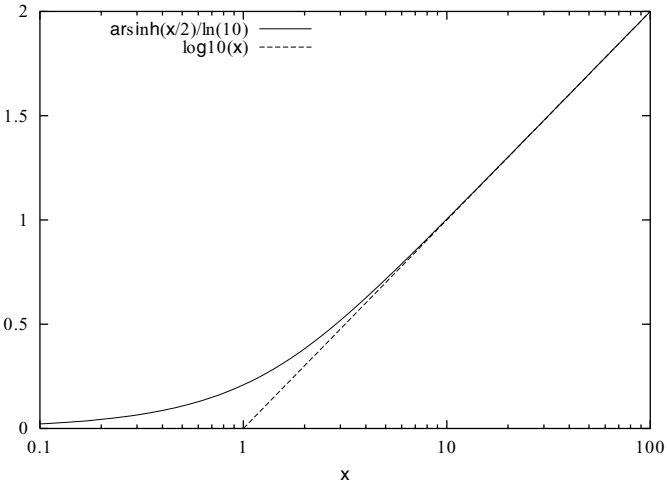

Fig. 2. The function $y = \mathrm{Ash}_{10}(x) \equiv \mathrm{Arsinh}(x/2)/\ln(10)$ represents data with positive and negative signs over a large range of scales, in comparison with the common $y = \log_{10} x$

i.e. for the first terms

$$F_2 = \frac{4}{3}, \quad F_3 = \frac{9}{4}, \quad F_4 = \frac{208}{45}, \quad F_5 = \frac{2425}{216}, \quad F_6 = \frac{2207}{70}. \tag{23}$$

Therefore, with increasing energy more and more moments F_q are needed to represent the multiplicity distribution.

Alternatively, one can study the ratios $H_q = K_q/F_q$ of cumulant and factorial moments. An intesting feature of these ratios is their asymptotic decrease with rank q [22]

$$H_q \simeq 1/q^2. \tag{24}$$

This behavior can be derived easily in leading order of $\gamma_0 \sim \sqrt{\alpha_s}$ under the assumption of constant K_q and F_q from the equation $k_q'' = \gamma_0^2 f_q$, which follows from (7) and (11) using (17).

On the other hand, these ratios are not very convenient near threshold. First, we can derive for the cumulant mo-

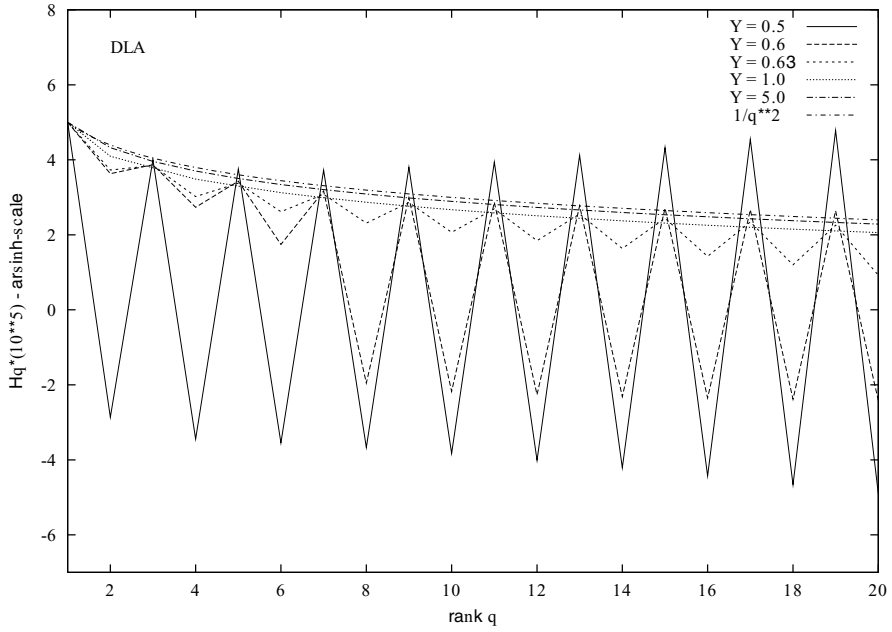

Fig. 3. Moment ratios H_q as function of rank q in DLA for different energies Y for fixed $Q_c = Q_0$ (representing hadrons). The quantity plotted is $\mathrm{Ash}_{10}(H_q \times 10^5)$ with function (27). With increasing Y the moments approach the asymptotic behavior $H_q \sim 1/q^2$

ments from (5) and (21)

$$K_q = (-1)^{q-1}(q-1)! \quad \text{for } Y_c = 0. \tag{25}$$

Then, because $F_q = 0$ for $q > 1$, the ratios H_q diverge in the limit $Y_c \to 0$ with alternating signs. Note that the observables F_q, K_q, H_q each provide a full description of the multiplicity distribution. At high energies K_q and H_q are convenient, whereas at low energies F_q is more convenient since the respective higher order terms are suppressed.

Before we come to a discussion of the results, we introduce a convenient way to present data with a large range of scales and alternating signs. It is an extension of the usual log plot for positive numbers in which a positive quantity y is represented in log scale $y = 10^x,\ x = \log_{10} y$. For a quantity with either sign we write

$$y = 10^x - 10^{-x} = 2\mathrm{Sinh}(x \ln 10), \tag{26}$$

$$x := \mathrm{Ash}_{10}(y) = (1/\ln 10)\mathrm{Arsinh}(y/2), \tag{27}$$

where $\mathrm{Arsinh}(z) = \ln(z + \sqrt{1+z^2})$. For large positive or negative numbers one obtains $\mathrm{Ash}_{10}(\pm y) \approx \pm \log_{10}(y)$ For convenience we show in Fig. 2 the comparison of both functions.

First, we study the evolution of the ratios, H_q, with energy $Y = \ln(E/Q_0)$ and this is shown in Fig. 3 for a few values of Y. One can see the oscillations with large amplitude near threshold (small Y) which follow from (25). With increasing energy the oscillations continue with the same oscillation length but with decreasing amplitude. The moments of even rank q finally change sign and the oscillations disappear at $Y = 1$ where they are already close to the asymptotic limit (24). Also one observes the rise of H_q with q at small Y and the decrease of H_q with q at large Y.

Next we present in Fig. 4 the evolution of the ratios H_q with energy Y which diverge at threshold and approach the asymptotic result (24) from below. At the same time we show the variation of the multiplicity moments for jets at variable resolution at fixed energy $Y = 5$ (corresponding to LEP energies at $Q_0 \approx 0.3\,\mathrm{GeV}$). Similarly to the case of multiplicity, there is a large difference between both dependences, which reflects again the role of the running coupling. The rise of the jet moments is delayed but they reach the hadron moments as $Q_c \to Q_0$ at the nominal energy of $Y = 5$.

Finally we remark that the comparison with e^+e^- results would require quark jets in two hemispheres. This can be obtained [3] by replacing the generating function as follows:

$$Z \ \to \ Z^{2C_F/C_A} = Z^{8/9}. \tag{28}$$

We do not go into this minor difference in the present qualitative discussion.

3.2 Modified leading logarithmic approximation

In this approximation, the full DGLAP splitting functions [37,38] are included, with energy conservation taken into account. The restriction to 1-loop results remains. MLLA takes into account the next-to-leading order terms in the $\sqrt{\alpha_s}$ expansion of the exponent, $\ln N_g$. In the present analysis, we neglect the $q\bar{q}$ pair production (even though it contributes in MLLA) for simplicity – it could be taken into account without difficulty (see, for example [16,17]). The

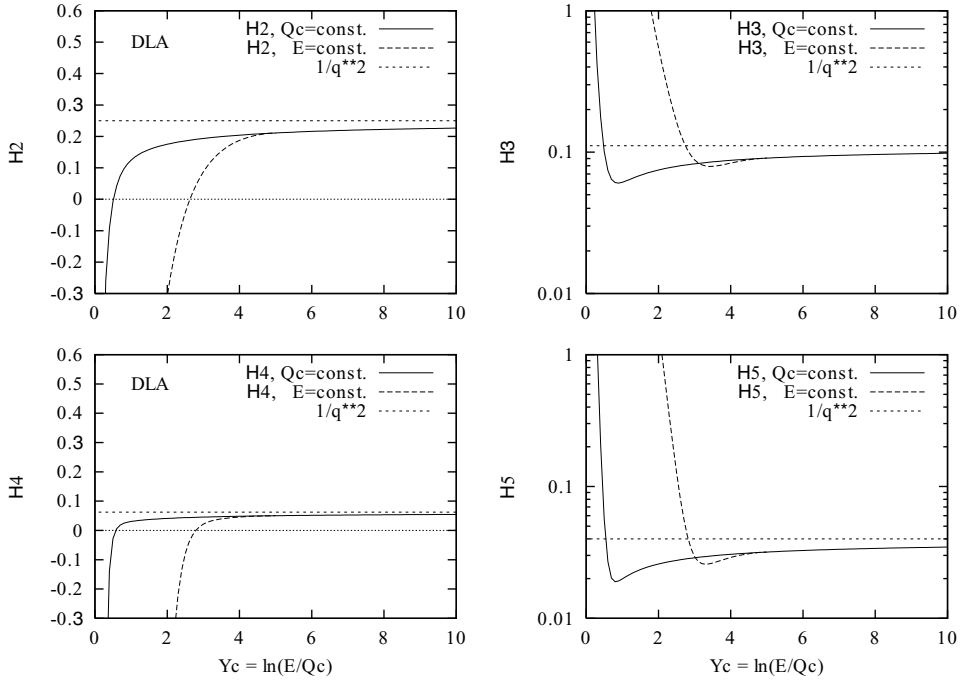

Fig. 4. Ratios of moments H_q in DLA versus energy for fixed $Q_c = Q_0$ (representing hadrons) and for fixed energy $Y = \ln(E/Q_0) = 5$ but variable Q_c representing jets at variable resolution $y_{cut} = (Q_c/2E)^2$. The asymptotic limits $H_q \to 1/q^2$ are shown as well

evolution equation for the generating function $Z(Y_c, u)$ in gluodynamics reads [15]

$$\frac{\mathrm{d}Z(Y_c,u)}{\mathrm{d}Y_c} = \int_{z_c}^{1-z_c} \mathrm{d}z \frac{\alpha_s(\tilde{k_T})}{2\pi} P_{gg}(z) \tag{29}$$

$$\times\{Z(Y_c + \ln z, u)Z(Y_c + \ln(1-z), u) - Z(Y_c, u)\},$$

$$Z(0, u) = u, \tag{30}$$

where

$$z_c = \mathrm{e}^{-Y_c}, \quad \alpha_s(\tilde{k_T}) = \frac{2\pi}{b\,\ln(\tilde{k_T}/\Lambda)}, \quad \tilde{k_T} = \min(z, 1-z)E, \tag{31}$$

and the splitting function $P_{gg}(z)$ is given by[1]

$$P_{gg}(z) = 6\left[z(1-z) + \frac{1-z}{z} + \frac{z}{1-z}\right]. \tag{32}$$

For the symmetric kernel one can replace in the integral $\frac{1}{2}P_{gg}(z)$ by $P_{gg}^{\mathrm{asy}}(z) = (1-z)P_{gg}$ which has no pole at $z = 1$ and behaves for $z \to 0$ like $P_{gg}^{\mathrm{asy}} \sim 6/z$. Differentiation by u leads again to evolution equations for the multiplicity N_g

$$N_g'(Y_c) = \int_{z_c}^{1-z_c} \mathrm{d}z \frac{\alpha_s(\tilde{k_T})}{\pi} P_{gg}^{\mathrm{asy}}(z) \tag{33}$$

$$\times\{N_g(Y_c + \ln z) + N_g(Y_c + \ln(1-z)) - N_g(Y_c)\}$$

and the unnormalized factorial moments

$$f_q'(Y_c) = \int_{z_c}^{1-z_c} \mathrm{d}z \frac{\alpha_s(\tilde{k_T})}{\pi} P_{gg}^{\mathrm{asy}}(z) \tag{34}$$

$$\times\{f_q(Y_c + \ln z) + f_q(Y_c + \ln(1-z)) - f_q(Y_c)$$

$$+ \sum_{m=1}^{q-1} \binom{q}{m} f_m(Y_c + \ln z) f_{(q-m)}(Y_c + \ln(1-z))\Bigg\}.$$

At threshold for multiparticle production, we find the following conditions

$$q = 1: \quad N_g = 1 \text{ for } E \le 2Q_c,$$

$$q > 1: \quad f_q = 0 \text{ for } E \le qQ_c. \tag{35}$$

The condition for $q = 1$ follows from the initial condition $N_g = 1$ and $N_g' = 0$ in (33) below the threshold for particle emission at $E \le 2Q_c$.

The constraint for the higher moments, f_q for $E < qQ_c$, corresponds to the kinematic condition for producing q particles. We can derive the condition for $q > 1$ by induction. First, consider the case of $q = 2$ in (34). We know that $f_2(Y_c) = 0$ if $Y_c \le \ln 2$ (equivalently, if $E \le 2Q_c$) from $f_1 \equiv N = 1$ in this region. Now let us consider the situation for $q > 2$, taking (35) for $q-1$ as given. Consider first the evolution of $f_q(Y_c)$ in (34) with Y_c starting from $f_q = 0$ at $Y_c \le \ln 2$ where $N = 1$. As long as the sum in (34) vanishes we just have the evolution $f_q'(Y_c) = f_q(Y_c) \times I(Y_c)$ with a known integral I and therefore $f_q = 0$.

[1] The P function [37] is related to the Φ function [38] by $\Phi_{ab} = 2P_{ab}$

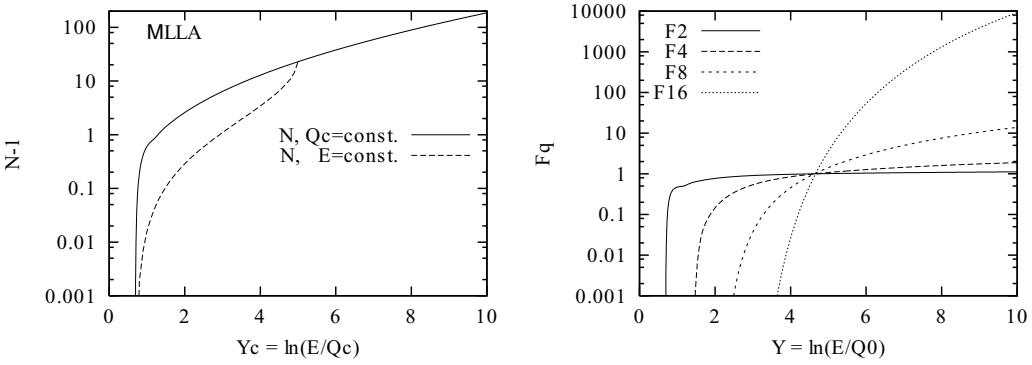

Fig. 5. Multiplicity N in DLA in single jet versus energy for fixed $Q_c = Q_0$ (representing hadrons) and for fixed energy $Y_0 = \ln(E/Q_0) = 5$ but variable Q_c representing jets at variable resolution Q_c (or $y_{cut} = (Q_c/2E)^2$) and factorial moments F_q versus energy Y_0

Next we show that for energies $E \leq qQ_c$ (or $Y_c < \ln q$) this sum indeed vanishes. First, note that the argument $\ln(zE/Q_c)$ of the moment f_m varies from 0 at the lower limit to $\ln(q-1)$ at the upper limit, while z varies from z_c to $1-z_c$ and the argument of $f_{(q-m)}$ decreases from $\ln(q-1)$ to 0. In the sum, exactly one of the factors – f_m at energy $E' = zE$ or f_{q-m} at energy $E'' = (1-z)E$ – vanishes because of condition (35) for $m < q$ or $q - m < q$

$$E' < mQ_c, \;\; E'' > (q-m)Q_c, \;\; f_m = 0, \;\; f_{q-m} \geq 0, \quad (36)$$

$$E' > mQ_c, \;\; E'' < (q-m)Q_c, \;\; f_{q-m} = 0, \;\; f_m \geq 0. \quad (37)$$

Now the perceptive reader may notice that for $m = 1$, $f_m = N_g$ cannot be 0. This is no problem, however, since $f_{q-1} = 0$ in the whole range. Thus, we have proven the validity of (35) for any q.

The MLLA evolution equation (29) reduces to the DLA equation (11) if the integrand is taken in the small z approximation, i.e. the $\ln(1-z)$ term is neglected and $P_{gg}(z) \sim 1/z$. This limit should be achieved for very high energies, because $\alpha_s(\tilde{k}_T)$ remains energy independent and gives weight to ever smaller values of z under the integral. Indeed, the high energy results for the moments in terms of an $\sqrt{\alpha_s}$ expansion [11,22] yields the DLA solutions in the asymptotic limit.

Full solutions of the evolution equations (33) and (34) satisfying the threshold condition, analogous to (18) in DLA are not known. If the integrand is simplified assuming a $\sqrt{\alpha_s}$ expansion one obtains expressions with Bessel functions similar to (18) but with non-integer index [9,39] which remain finite for $Q_0 \to \Lambda$.

Here we solve the system of equations (33) and (34) again numerically using the trapezoidal approximation with step size 10^{-3} for the integral (for control also with 10^{-2}); alternatively, the 3-point Simpson rule has been applied with similar results. Note that the evolution variable $Y_c \sim \ln E$ now not only appears in the integration limits but also in the integrand, which was not the case in the DLA.

In Fig. 5 we show the numerical results for the multiplicity N in a single jet as function of Y_c for hadrons (fixed $Q_c = Q_0$ according to LPHD) and for jets at fixed energy E (LEP energy) but variable resolution. The results look similar to Fig. 1 in DLA, but the absolute size is now much reduced because of the energy conservation constraint.

Also shown are some factorial moments, F_q. Again, the moments are smaller in size and, therefore, the approach to the asymptotic values (23) is further delayed. A distinctive difference from DLA are the shifted threshold energies for the higher moments according to (35).

The factorial moments F_q show a striking result at intermediate energies: they all cross at one point ($E \approx 20\,\mathrm{GeV}$) with $F_q = 1$, i.e. with a Poissonian distribution:

Poissonian transition point:

$$F_q = 1 \qquad \text{at} \qquad Y_P \approx 4.7. \quad (38)$$

This feature does not appear in DLA, and is apparently related to the delayed thresholds. For the considered moments with $q \leq 16$ the crossing at $F_q = 1$ occurs within an interval of $\delta Y \approx 0.05$ for both step sizes 10^{-3} and 10^{-2} of our numerical computation, so the distribution is close to a Poissonian. We note, though, that the higher moments F_q with $q \gtrsim 32$ have a threshold above the transition point Y_P so the Poissonian cannot be an exact solution. Nevertheless, it is remarkable that besides the threshold and asymptotic regime, there is an intermediate energy with a very simple behavior. The Poissonian transition point follows apparently from the evolution equation – a novel property for which we have no analytical explanation yet.

Next we consider the moment ratios H_q for hadrons ($Q_c = Q_0$) from low to high energies in Fig. 6. At the low energies ($Y \leq 4$) we observe again the pattern of rapid oscillations from one order q to the next as in DLA reflecting the threshold behavior. Beyond the Poissonian transition point ($Y \geq 6$) we enter a new regime with a larger oscillation length. The first minimum is slowly rising from $q = 5$ at $Y = 6$ to $q = 7$ at $Y = 10$. At higher q a maximum follows. This is expected from the analytical results [13,22]. Whereas the oscillation amplitude of H_q rises with q at low energies, it decreases at the high energies. However, it is always much below the asymptotic DLA limit for large q, only for small q below the first minimum one can see a convergence to this limit in the considered energy range.

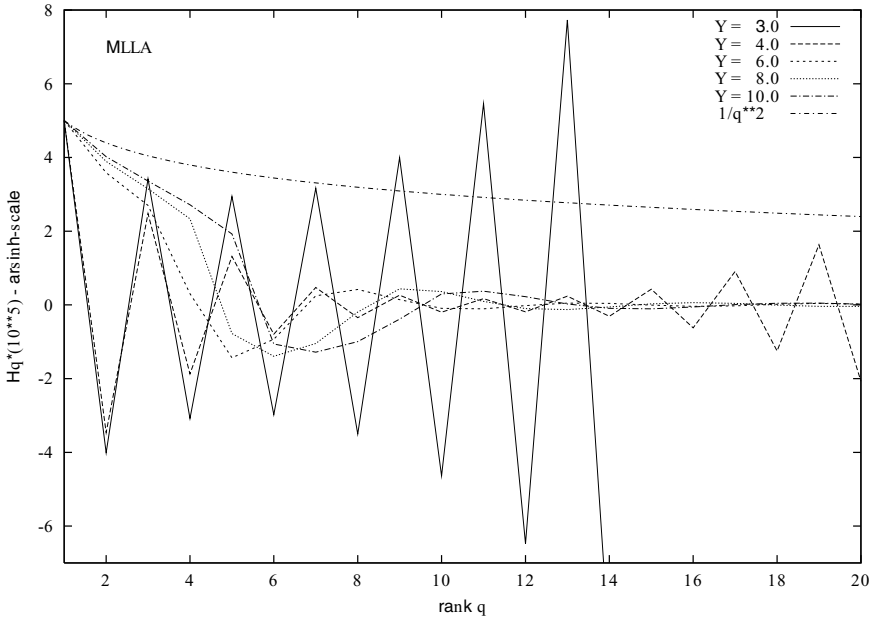

Fig. 6. Moment ratios H_q as function of rank q in MLLA for different energies Y for fixed $Q_c = Q_0$ (representing hadrons). With increasing Y the moments approach the asymptotic behavior $H_q \simeq 1/q^2$

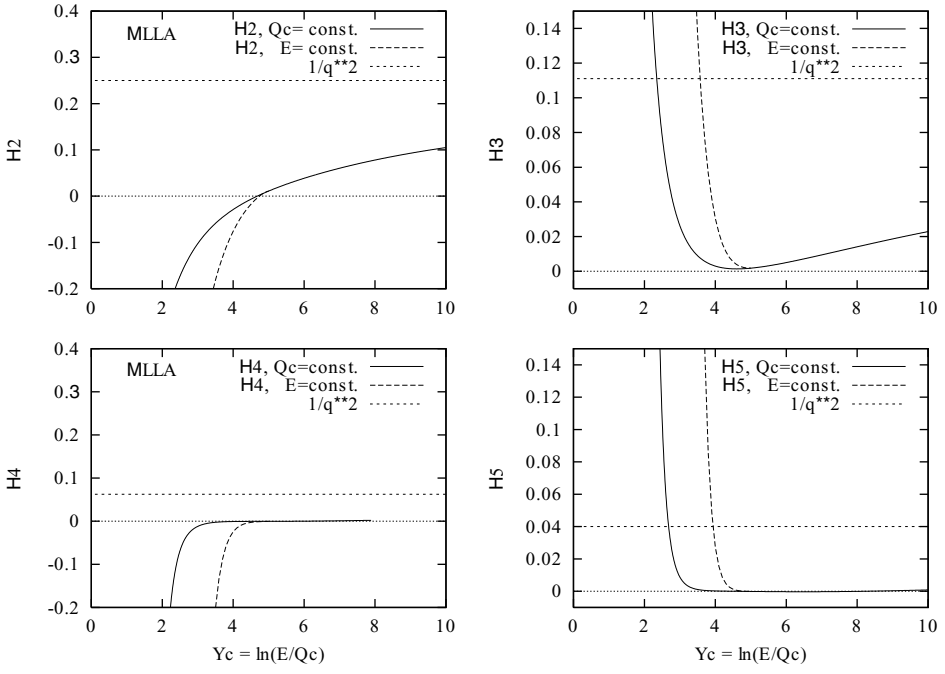

Fig. 7. Ratio of moments H_q in MLLA versus energy for fixed $Q_c = Q_0$ (representing hadrons) and for fixed energy $Y = \ln(E/Q_0) = 5$ but variable Q_c representing jets at variable resolution $y_{cut} = (Q_c/2E)^2$. The asymptotic limits $H_q \to 1/q^2$ are shown as well

The evolution of the H_q moments with Y_c is shown in Fig. 7 for hadrons and jets. In comparison to the DLA results of Fig. 4, we see at first a qualitatively similar behavior, but again the approach to the asymptotic limit is not visible for the higher moments in the considered energy range.

More details are shown for hadrons in Fig. 8. New features emerge at high energies (above $Y \approx Y_P \approx 4$). For the higher moments ($q \geq 4$) secondary minima and/or maxima appear with increasing energy at the level of $\mathcal{O}(10^{-4})$. These secondary oscillations lead to a delay of the onset of the asymptotic behavior. Below $Y_c = 20$ ($E \lesssim 10^8$ GeV) the moments with $q \geq 6$ are below 1/10 of their DLA asymptotic value.

The Poissonian transition point corresponds to $H_q = 0$ for all $q > 1$. Indeed the moments show this behavior in

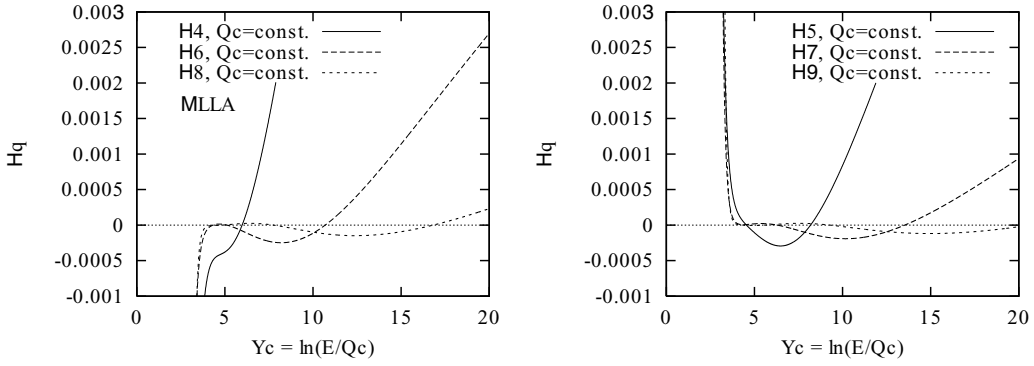

Fig. 8. Moment ratios H_q in MLLA versus energy for fixed $Q_c = Q_0$ (representing hadrons) as in Fig. 7. The asymptotic limits of H_q are above the upper bound of the plot

good approximation at the above Y_P. Beyond this point the positive short range correlations lead to a positive H_2, whereas below it the energy conservation constraints lead to a negative cumulant. In general, the even H_q ratios change sign because of the negative value at threshold and the positive $1/q^2$ asymptotic limit. In hadron phenomenology, the positive correlations $H_2 > 0$ reflect the resonance production [40], in our calculation it is the gluon bremsstrahlung with small angle (above Q_0 cut-off) which lead to the short range correlations, be it between "hadrons" (partons at scale Q_0) or between (mini) jets.

As common features of DLA and MLLA, we note the splitting between hadron and jet moments at the same Y_c which is a direct consequence of the running coupling. Hadron and jet multiplicities coincide for $Q_c \to Q_0$.

4 Monte Carlo simulation of parton cascade

After the numerical solutions of the DLA and MLLA evolution equations for single jets, we finally apply an MC event generator (ARIADNE [32]) at the parton level based on the same procedures as the above evolution equations: perturbative QCD evolution with the coupling $\alpha_s(k_T)$ terminated by a transverse momentum, k_T, cut-off and arbitrary parameters Λ and $Q_0 > \Lambda$. The MC involves the coupled evolution of quarks and gluons in the cascade, the inclusion of large angle radiation, the full first-order matrix element for $e^+e^- \to q\bar{q}g$, and exact energy-momentum conservation. These features lead to a higher accuracy than our MLLA calculation.[2] On the other hand, a simplification of the Monte Carlo is the exclusive use of 1-loop calculations. This simplification could result in deviations when very different energy scales are compared.

In our adoption of the MC program, we set all quark masses to zero but kept the masses for heavy quarks in the calculation of the number of flavors n_f for α_s at a given dipole mass. The results depend only on the two adjustable parameters Λ and Q_0; alternatively, we use the parameter $\lambda = \ln(Q_0/\Lambda)$. These parameters have been determined from a fit to multiplicities. We refer to this modified Monte Carlo as "ARIADNE-D," where "D" stands for "Duality".

The jet multiplicities are obtained from the final state partons using the Durham algorithm, just as in the experimental analysis with (8) and (9). Hadron multiplicities are related to the parton multiplicities, generated at scale Q_0, according to the LPHD prescription.

This model will be compared with the experimental data. First we consider the mean hadron and jet multiplicities N, as shown in Fig. 9. The jet multiplicities for energies $Q = 35$, 91 and 189 GeV are obtained as functions of the cut-off Q_c or of $y_{cut} = (Q_c/Q)^2$ – in the figure they are plotted as a function of the variable

$$Y_{cs} = -\frac{1}{2}\ln(y_{cut} + Q_0^2/Q^2) = \frac{1}{2}\ln(Q^2/(Q_c^2 + Q_0^2)) \quad (39)$$

with the additional scale Q_0. The MC parton multiplicity N_{part} is shown at the cut-off $Q_c = Q_0$ and should be compared at this scale with the total hadron multiplicity N_{tot} according to the LPHD prescription, in general $N_{tot} = K \times N_{part}$ (where K is a constant); the observed charged multiplicity is given by $N_{ch} = f_{ch}N_{tot}$ with the charged particle fraction f_{ch}. These factors also depend on whether weak and electromagnetic decays of hadrons are included ($K^0, \Lambda, \ldots$). The factor Kf_{ch} will be determined from the fit. A simple choice is $K = 1$ as for jets and $f_{ch} = 2/3$ as obtained previously [16].[3] For jets we compare parton and hadron results at the same cut-off and with $K = 1$. Note that the choice of variable does not matter for the comparison of jet properties (both MC and experimental data are obtained by the same procedure); but, using the variable Y_{cs} in (39), has the advantage that the jet data approach the hadron data for $y_{cut} \to 0$ at a finite value of Y_{cs} in the figure according to (9). In the region $Q_c =$ 1–2 GeV the dependence on Q_0 disappears and we are in the perturbative QCD regime, governed by the single parameter Λ [52].

[2] In MLLA, the inclusion of quark jets is possible – also, the first-order matrix element has been included in the calculation of multiplicities [16], however, energy-momentum conservation is fully realized in the MC approach and large angle emission is more easily accessible.

[3] If proportionality of energy spectra of partons and hadrons according to LPHD is required in the full energy range, then the normalization has to be the same ($K = 1$) because of energy conservation.

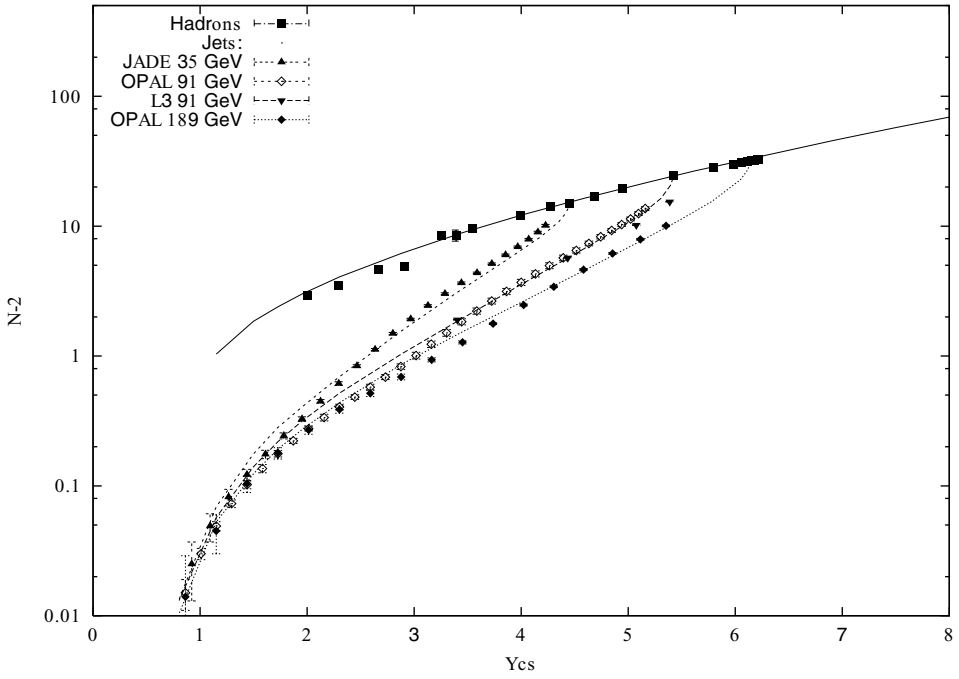

Fig. 9. Multiplicity N of hadrons (taken as $N_{\rm ch} \times 1.25$ using data [41–50] and LEP averages from [22]) and multiplicity of jets [51,28] in e^+e^- annihilation together with our Monte Carlo calculations as function of $Y_{\rm cs}$; see (39) ($Y_{\rm cs} \sim \ln(Q/Q_{\rm c})$)

Table 1. Monte Carlo results on hadron and jet multiplicities for given values of Λ (rows) and λ (columns). The first half of the table consists of data with $y_{\rm cut} = 0$ (hadrons), and the second half consists of data with $y_{\rm cut} = 2 \times 10^{-5}$

Λ(MeV)	$\lambda = 0.001$	$\lambda = 0.01$	$\lambda = 0.015$	$\lambda = 0.05$
250	35.8	31.7	30.6	26.5
300	33.3	29.5	28.4	24.8
400	29.6	26.3	25.4	22.0
500	27.0	24.0	23.2	20.1
250	12.4	12.2	12.1	11.8
300	13.0	12.8	12.7	12.4
400	13.9	13.6	13.5	13.0
500	14.4	14.0	13.9	13.2

In order to determine the parameters of the model we compared the MC results with the multiplicity data at LEP-1. We noted that we could not get good agreement with the jet data from OPAL [51] over the entire kinematic range of $10^{-5} < y_{\rm cut} < 0.5$. Since we were interested in studying the transition between jets and hadrons, we chose our parameters so that they gave a particularly good description of the low $y_{\rm cut}$ regime and the hadron multiplicity as well as the very large $y_{\rm cut}$ region. In Table 1 we illustrate the dependence of the hadron and jet multiplicity on the parameters. We require a good fit of the jet multiplicity of $N = 14.1 \pm 0.4$ for $y_{\rm cut} = 2 \times 10^{-5}$ [51] corresponding to $Q_{\rm c} = 0.4\,{\rm GeV}$. At this scale the particles from non-hadronic decays are recombined into the primary hadrons and this ambiguity is removed. Also we considered the mean charged multiplicity at LEP-1 of $N_{\rm ch} = 21.2 \pm 0.3$ [22] (this number includes particles from K^0 and Λ decays). Solutions can be found close to the simple case $f_{\rm ch} K = 2/3$. We do not require this condition though and choose the parameters

$$\Lambda = 400\ {\rm MeV}, \quad \lambda = 0.01, \quad (K f_{\rm ch})^{-1} = 1.25; \qquad (40)$$

they are not very different from the previous study for hadrons alone ($\Lambda = 200\,{\rm MeV}$, $\lambda = 0.015$ and $(K f_{\rm ch})^{-1} = 1.5$ [53]) which optimized the description of the hadronic correlations alone.

With our choice (40) a reasonable description of jet multiplicities for small and large $y_{\rm cut}$ was obtained, not only at LEP-1, but also at the higher and lower energies of 35 and 189 GeV, as can be seen in Fig. 9. Furthermore we get a good description of the trend of hadron multiplicities as function of CMS energy in the full range $Q = 3$–$200\,{\rm GeV}$. The Monte Carlo was run with 250 000 events at each energy.

As in the analytic calculations, the multiplicity in the MC approach applied here would diverge for $Q_0 \to \Lambda$. Now, Fig. 9 shows that with the same cut-off Q_0 taken at all energies the correct energy dependence of the hadron multiplicity is obtained.

At every CMS energy in Fig. 9, the MC fails to reproduce the intermediate $y_{\rm cut}$ region with MC results falling above the experimental data. We find that the structure we are unable to reproduce occurs at the fixed b mass scale $Q_{\rm c} \sim 5\,{\rm GeV}$ at all energies. In our Monte Carlo we use only light quarks so as to avoid complicated decay processes. It is plausible to assume, then, that the "hump" structure at 5 GeV comes from b quark production. This conjecture is further supported by the enhancement of the effect seen at the Z energy of 91 GeV as expected from the enhanced

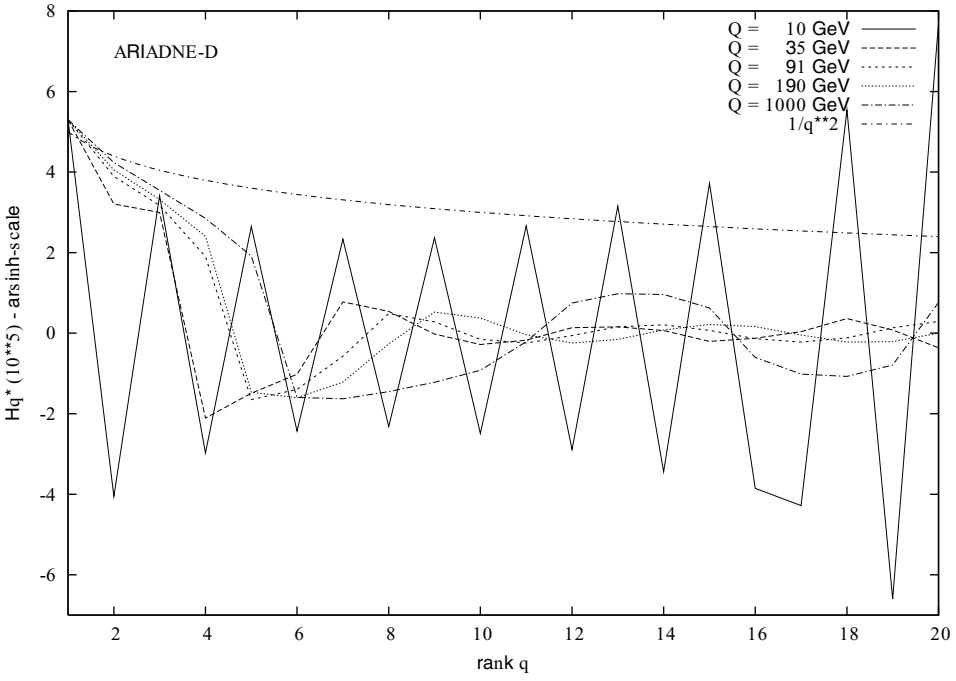

Fig. 10. Ratios H_q for a sequence of CMS energies Q in e^+e^- annihilation as obtained from the Monte Carlo calculation, plotted as in Fig. 3

b quark production by neutral current interactions of the Z.

The results in Fig. 9 look similar to the analytic solutions in Figs. 1 and 5 and demonstrate again the importance of the running coupling which leads to the scale (Q) dependence of multiplicity at fixed $Y_{\rm cs}$ or $Q/Q_{\rm c}$; in the threshold region (low $Y_{\rm cs}$) the difference between hadron and jet multiplicities amounts to a an order of magnitude.

Next, we turn to the energy evolution of the H_q moments for hadrons (i.e. partons at scale Q_0) from low to high energies (10–1000 GeV). This evolution is displayed in Fig. 10 and looks similar to the result from MLLA in Fig. 6: at the low energy, below the Poissonian point, there are the rapid oscillations reflecting the threshold behavior, above that point we observe the oscillations with increasing length for increasing energy. The first minimum occurs at $q_{\rm min} \approx 5$ at 90 GeV and increases to $q_{\rm min} \approx 7$ at 1000 GeV. This increase is similar but a bit stronger than in the asymptotic formula (3), which would predict an increase by one unit of $q_{\rm min}$ instead of two. These calculations have been carried out with a sample of 4 M events. The statistical errors are determined from the fluctuations of 4 sub-samples and are found to be significantly smaller than the oscillation amplitudes at their maximum. The numerical results are also given in Table 2.

In Fig. 11, we compare the ratios, H_q, obtained from our calculations with the measurements by L3, both for hadrons and for jets with variable (Durham) cut-off $Q_{\rm c}$. For hadrons we assume that the multiplicity distribution of charged particles has the same normalized moments as the distribution of all particles. This is the case if the same conversion factor $f_{\rm ch}$ applies for all multiplicities n.

For hadrons, a measurement of the full multiplicity distribution [29] which extends up to $n_{\rm ch} = 62$ and one with truncation [28] at the multiplicity $n_{\rm ch} = 48$ are presented. The truncation can be seen to considerably increase the oscillation amplitude. We compare with the Monte Carlo results again with and without truncation. The truncation was at multiplicity $n_{\rm t} = 63$ to obtain the same event fraction of 0.005% for multiplicities $n > n_{\rm t}$ as in the experimental data. Our results reproduce the data rather well but for the truncated moments the high q oscillations are a bit weaker.

We mention here another subtlety of the experimental analysis. The L3 data in Fig. 11 refer to data without K^0 and Λ decays, whereas the multiplicities in Fig. 9 include them. However, the H_q moments do not depend on this difference, except to within a few per cent. The same is true for the truncated moments, as long as the removed event fraction is the same [29]. This appears to be plausible from the point of view of KNO scaling.

We note that the moments presented by the SLD Collaboration [27] have been determined from the multiplicity range $6 \le n_{\rm ch} \le 54$ and they look very similar to the truncated L3 moments. We stress that from our point of view the untruncated moments are of primary relevance; only these obey the evolution equations discussed above and have simple asymptotic properties. Beyond the first minimum they are very small at LEP energies, of the order of 10^{-5}.

Finally, in the same figure, Fig. 11, we study the evolution of the H_q moments with cut-off $Q_{\rm c}$ or $y_{\rm cut} = (Q_{\rm c}/Q)^2$. The MC calculations reproduce well the change from the rapid oscillations with large amplitude at large cut-off $Q_{\rm c}/Q$ to the oscillations with larger oscillation length and

Table 2. Ratios of multiplicity moments, H_q, for different CMS energies, Q, in e^+e^- anihilation obtained from ARIADNE-D parton MC (the statistical errors of the MC results are generally smaller than the last digit given)

q	10 GeV	35 GeV	91 GeV	190 GeV	1000 GeV
2	−0.0565	0.00808	0.039	0.0569	0.0864
3	0.0129	0.00495	0.0074	0.0104	0.0176
4	−0.0047	−0.00064	0.00040	0.00126	0.00356
5	0.0022	−0.00015	−0.00022	−0.00014	0.00040
6	−0.0013	−0.000051	−0.00012	−0.00020	−0.00019
7	0.0010	0.000028	−0.000017	−0.00008	−0.00021
8	−0.0010	0.000015	0.000013	−0.000006	−0.00014
9	0.0011	−0.0000005	0.000006	0.000015	−0.00008
10	−0.0015	−0.0000069	−0.000003	0.000009	−0.00004
11	0.0022	−0.0000041	−0.000005	−0.0000009	−0.000005
12	−0.0038	0.0000032	−0.000001	−0.000005	0.000027
13	0.0071	0.0000036	0.000003	−0.000003	0.000047
14	−0.013	0.0000014	0.000004	0.000001	0.000045
15	0.026	−0.0000048	0.000001	0.000005	0.000019
16	−0.035	−0.0000029	−0.000003	0.000003	−0.000018
17	−0.09	0.0000008	−0.000005	−0.000001	−0.00005
18	1.7	0.0000093	−0.000002	−0.000005	−0.00005
19	−19	0.0000018	0.000003	−0.000005	−0.00003
20	250	−0.0000093	0.000007	0.000001	0.00002

smaller amplitudes in the small Q_c/Q region close to the fully resolved hadronic final state.

In the subsequent Figs. 12–14 we show these ratios, H_q, separately as function of Y_{cs}, i.e. of Q/Q_c. Included are further data at intermediate y_{cut} values from [29] together with the corresponding MC predictions and also the predictions for the hadronic final state, i.e. at $Q_c = Q_0$. In these calculations 2.5 M events have been generated in the MC. For all orders q, the calculation follows the experimental data closely. Again, there is the same qualitative difference between the hadron and jet data as observed before for the DLA and MLLA calculations in Figs. 4 and 7.

For the ratio H_2 we also compare with results we deduced from TASSO moments [54]. The data clearly confirm the splitting of the moments at different scales, as expected from the running coupling. At small Q/Q_c, both for hadrons and for jets, the distribution is narrower than Poisson ($H_2 < 0$), while at higher values of this ratio the distribution gets broader ($H_2 > 0$). The positive H_q is expected from the short range correlations, either from gluon bremsstrahlung at small angles for partons or from resonance decays for hadrons. At the point with $H_2 = 0$ the higher moments are also close to zero corresponding to a Poissonian transition point, both for jets and hadrons:

Poissonian transition point:

$$\begin{array}{ll} Q \approx 30 \text{ GeV} & \text{hadrons}, \\ Q = 91,\ Q_c \approx 0.3\,\text{GeV} & \text{jets}. \end{array} \tag{41}$$

It is interesting to note that the Poissonian distribution has actually been successfully fit to the data at 29 GeV by the HRS Collaboration [45].

We observe again a close similarity between MC and MLLA results, although the deviations from a Poissonian ($H_3 > 0$ at minimum) appear a bit larger in the MC.

5 Conclusions

We have studied the multiplicity moments, in particular the H_q ratios for the QCD parton cascade in three different approximations: DLA, MLLA and parton Monte Carlo. The DLA predicts the very asymptotic behavior. The asymptotic MLLA corrections predict the existence of H_q oscillations but do not explain any y_{cut} dependence. The more precise calculations of the full MLLA solution of the evolution equations and the Monte Carlo method, which include the correct threshold behavior, show at the presently accessible energies the following new features of the multiplicity moments:

(a) There is a particular energy scale, Y_P, for hadrons or a particular y_{cut} for jets where the multiplicity distribution is approximately Poissonian ($H_q \approx 0,\ F_q \approx 1$ for $q > 1$).

(b) In a region of smaller energies there is a rapid oscillation of H_q, reflecting the threshold behavior; at higher energies the oscillation length increases with energy as predicted qualitatively by asymptotic MLLA, but the oscillation amplitude is much smaller. In fact, for hadrons at LEP energies we predict $|H_q| \lesssim 10^{-5}$ beyond the first minimum at $q \approx 5$. Also, there are secondary extrema of H_q

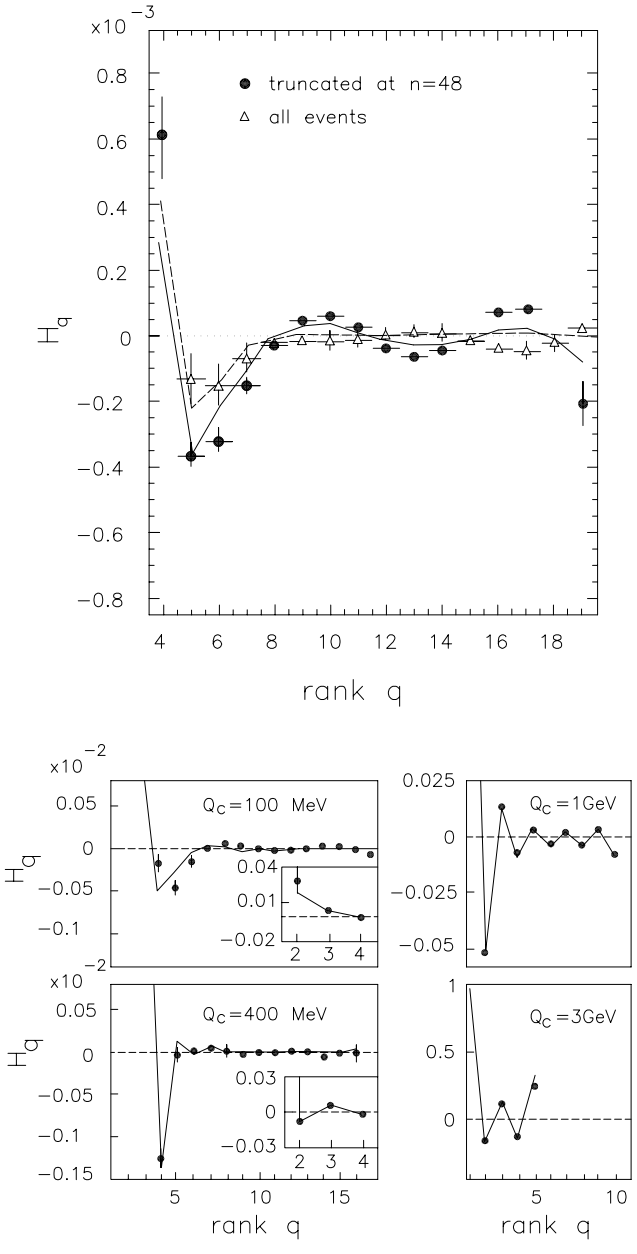

Fig. 11. (a) Ratio H_q of multiplicity moments obtained by L3 Collaboration [28,29] with truncation of multiplicity at $n_{\rm ch} = 48$ compared with ARIADNE-D MC (truncation at $n = 65$) and both without truncation; (b) ratios H_q for jets at different cut-off $Q_{\rm c}$ [28] compared with our MC results

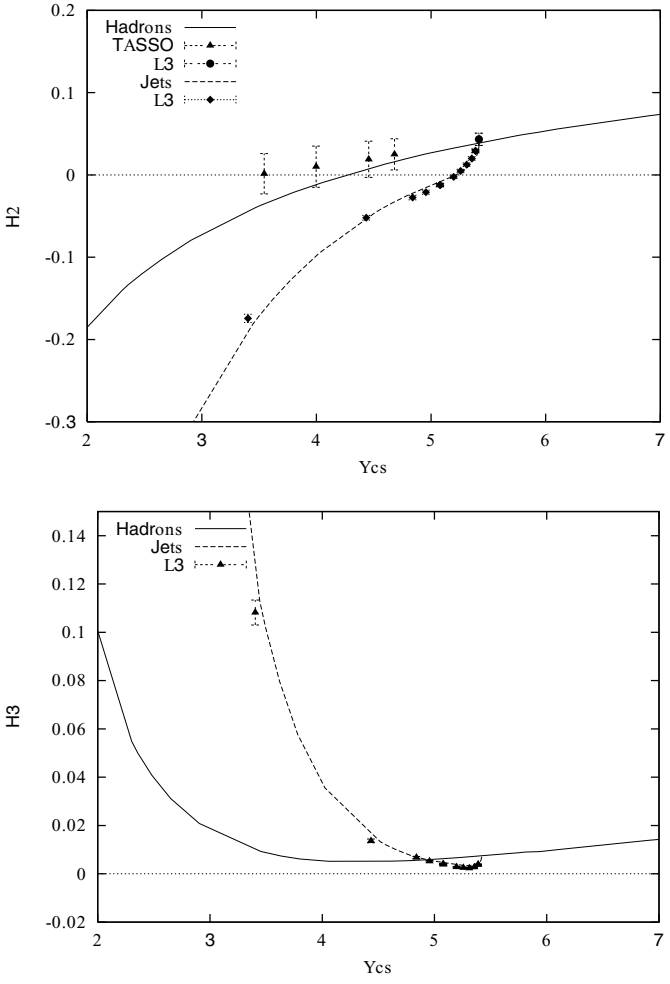

Fig. 12. Ratio of moments H_q for hadrons [54] and jets [28,29] in comparison with ARIADNE-D Monte Carlo

as a function of energy for a given rank q. The approach to the asymptotic DLA region is very slow if visible at all. (c) For fixed resolution parameter $y_{\rm cut}$ the moments of jets and hadrons are rather different as a consequence of the running coupling.

We conclude that the perturbative approach yields good results not only for single particle phenomena, such as single inclusive spectra and mean multiplicities, as envisaged originally in the LPHD approach, but also for correlations of high order. Above the Poissonian transition point, the short range correlations initiated by resonance decays for hadrons and gluon Bremsstrahlung for partons become increasingly important and lead to the broadening of the multiplicity distribution of both hadrons and jets ($H_2 > 0$). So there is a duality also between hadronic and partonic correlations.

Moreover, the absolute normalization, originally considered as free parameter, can be studied as function of resolution $y_{\rm cut}$ and a unified description of hadronic and jet phenomena is possible, using the variable $Y_{\rm cs}$ in (39) with the shifted $y_{\rm cut}$ prescription, both for multiplicities and correlations.

Both the predicted energy evolution of hadronic correlations and the $y_{\rm cut}$ dependence of the jet correlations follow the experimental results closely, with the exception of jets near the b quark threshold. In the jet regime $Q_{\rm c} \gtrsim 1$–$2\,{\rm GeV}$, the effect of the hadronic scale Q_0 becomes negligible and we are in the domain of perturbative QCD with the single parameter Λ only; $Q_{\rm c}$ is then an external parameter to be chosen by the experimenter. At smaller scales, the hadronic scale Q_0 becomes important, and the results become model dependent. The transition region from jets to hadrons for $y_{\rm cut} \to 0$, which shows strong variations of all moments, is very well reproduced by the

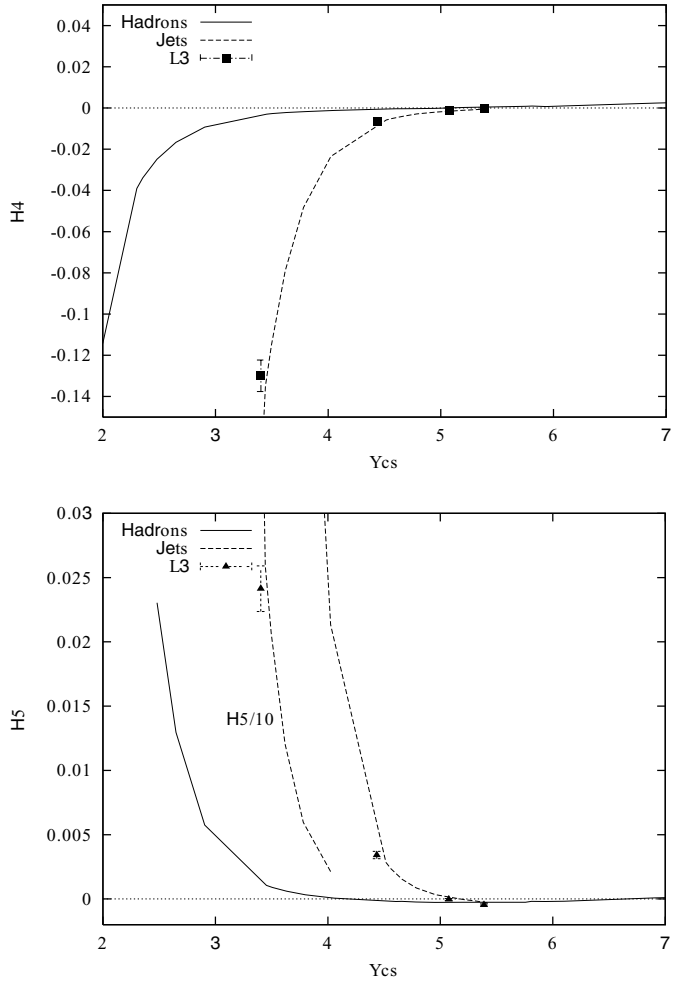

Fig. 13. Ratio of moments H_q for hadrons and jets as in Fig. 12

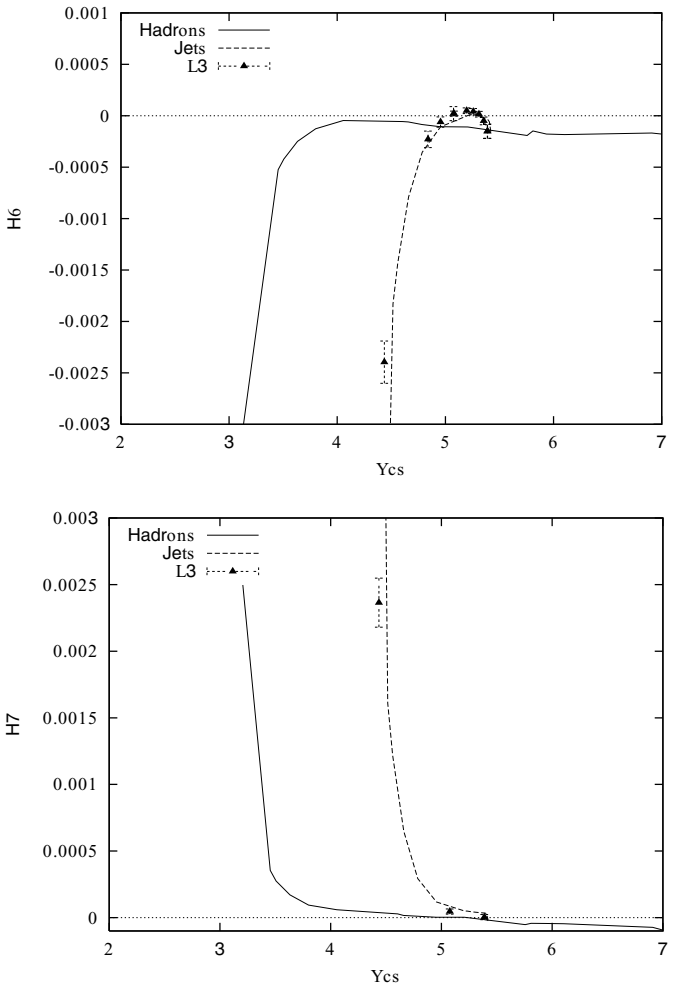

Fig. 14. Ratio of moments H_q for hadrons and jets as in Fig. 12

parton MC with low cut-off $k_{\mathrm{T}} \geq Q_0 > \Lambda$. In this region the coupling becomes large, i.e. $\alpha_{\mathrm{s}} \gtrsim 1$. An extension of the calculation into this kinematic region is not justified a priori, but, as seen from the analytical results, the convergence of the perturbation theory is not in danger, and the solutions can be obtained from the evolution equations or from the MC. This successful description can be viewed at least as a good effective parameterization of the soft transition region.

With increasing order, accurate calculations are required. So far, this is only accessible by numerical methods. Further improvements are possible by including heavy quarks in the parton evolution and by including the 2-loop results.

The good description of the data by the MC model with normalization $K \approx 1$ implies that in the considered applications, one parton counts for about one hadron and the hadron final state is well represented by a parton final state of the same multiplicity at resolution scale $Q_0 \gtrsim \Lambda$.

Acknowledgements. We thank Valery Khoze for the interesting discussions and useful comments on the manuscript.

References

1. W. Furmanski, R. Petronzio, S. Pokorski, Nucl. Phys. B **155**, 253 (1979)
2. A. Bassetto, M. Ciafaloni, G. Marchesini, Nucl. Phys. B **163**, 477 (1980)
3. Yu.L. Dokshitzer, V.S. Fadin, V.A. Khoze, Phys. Lett. B **115**, 242 (1982); Z. Phys. C **15**, 325 (1982)
4. B.I. Ermolayev, V.S. Fadin, JETP Lett. **33**, 285 (1981); V.S. Fadin, JETP Lett. **33**, 285 (1981)
5. A.H. Mueller, Phys. Lett. B **104**, 161 (1981)
6. A. Bassetto, M. Ciafaloni, G. Marchesini, A.H. Mueller, Nucl. Phys. B **207**, 189 (1982)
7. Yu.L. Dokshitzer, V.S. Fadin, V.A. Khoze, Z. Phys. C **18**, 37 (1983)
8. B.R. Webber, Phys. Lett. B **143**, 501 (1984)
9. Ya.I. Azimov, Yu.L. Dokshitzer, V.A. Khoze, S.I. Troyan, Z. Phys. C **27**, 65 (1985); Z. Phys. C **31**, 213 (1986)
10. A.H. Mueller, Nucl. Phys. B **213**, 85 (1983); Erratum B **241**, 141 (1984)
11. E.D. Malaza, B.R. Webber, Phys. Lett. B **149**, 501 (1984); Nucl. Phys. B **267**, 702 (1986)
12. J.B. Gaffney, A.H. Mueller, Nucl. Phys. B **250**, 109 (1985)

13. I.M. Dremin, Phys. Lett. B **313**, 209 (1993). I.M. Dremin, V.A. Nechitailo, Mod. Phys. Lett. A **9**, 1471 (1994)
14. A. Capella, I.M. Dremin, J.W. Gary, V.A. Nechitailo, J. Tran Thanh Van, Phys. Rev. D **61**, 074009 (2000)
15. Yu.L. Dokshitzer, V.A. Khoze, S.I. Troyan in Advanced Series on Directions in High Energy Physics – Perturbative Quantum Chromodynamics, edited by A.H. Mueller (World Scientific, Singapore 1989), Vol. 5, p. 241
16. S. Lupia, W. Ochs, Phys. Lett. B **418**, 214 (1998)
17. S. Lupia, Phys. Lett. B **439**, 150 (1988)
18. A. Giovannini, L. Van Hove, Acta Phys. Pol. B **19**, 495 (1988); B **19**, 917 (1988); M. Garetto, A. Giovannini, T. Sjöstrand, L. Van Hove, Proceedings Workshop on Multiparticle Dynamics (Perugia, Italy, June 1988) (World Scientific, Singapore 1989), p. 181
19. W. Ochs, T. Shimada, Rapidity gaps in quark and gluon jets, Proceedings XXIX International Symposion QCD & Multiparticle Production (ISMD99) (Providence, RI, USA, August 1999), edited by I. Sarcevic and Chung-I Tan (World Scientific, Singapore, 2000), p. 64, hep-ph/9911240, and to be published
20. Yu.L. Dokshitzer, V.A. Khoze, A.H. Mueller, S.I. Troyan, Basics of Perturbative QCD, edited by J. Tran Thanh Van (Editions Frontières, Gif-sur-Yvette 1991)
21. V.A. Khoze, W. Ochs, Int. J. Mod. Phys. A **12**, 2949 (1997); V.A. Khoze, W. Ochs, J. Wosiek, in Handbook of QCD, edited by M.A. Shifman (World Scientific, Singapore 2001), hep-ph/0009298
22. I.M. Dremin, J.W. Gary, Phys. Rep. **349**, 301 (2001)
23. Yu.L. Dokshitzer, QCD Phenomenology, CERN-Dubna School, Pylos, August 2002, hep-ph/0306287
24. OPAL collaboration, K. Akerstaff et al., Eur. Phys. J. C **1**, 479 (1998)
25. I.M. Dremin, B.B. Levtschenko, V.A. Nechitailo, Sov. J. Nucl. Phys. **59**, 1091 (1994)
26. CDF collaboration, T. Affolder et al., Phys. Rev. Lett. **87**, 211804 (2001)
27. SLD collaboration, K. Abe et al., Phys. Lett. B **371**, 149 (1996)
28. L3 collaboration, P. Achard et al., Measurement of the charged-particle multiplicity and inclusive momentum distributions in Z decays at LEP, hep-ex/0110072, October 2001
29. D.J. Mangeol, Correlations in the Charged-Particle Multiplicity Distribution, thesis University of Nijmegen, January 2002, hep-ex/0110029
30. R. Ugoccioni, A. Giovannini, S. Lupia, Phys. Lett. B **374**, 231 (1996)
31. R. Ugoccioni, A. Giovannini, S. Lupia, Phys. Lett. B **342**, 387 (1995)
32. L. Lönnblad, in Physics at HERA, Vol. **3**, 1440 (1991); L. Lönnblad, Comp. Phys. Comm. **71**, 15 (1992).
33. G. Gustafson, Phys. Lett. B **175**, 453 (1986)
34. Ya.I. Azimov, Yu.L. Dokshitzer, V.A. Khoze, S.I. Troyan, Phys. Lett. B **165**, 147 (1985); Sov. J. Nucl. Phys. **43**, 95 (1986)
35. N. Brown, W.J. Stirling, Phys. Lett. B **252**, 657 (1990); Z. Phys. C **53**, 629 (1992); S. Catani, Yu.L. Dokshitzer, M. Olsson, G. Turnock, B.R. Webber, Phys. Lett. B **269**, 432 (1991)
36. A. Bassetto, M. Ciafaloni, G. Marchesini, Phys. Rep. C **100**, 201 (1983)
37. G. Altarelli, G. Parisi, Nucl. Phys. B **126**, 298 (1977)
38. Yu.L. Dokshitzer, Sov. Phys. JETP **46**, 641 (1977)
39. S. Catani, Yu.L. Dokshitzer, F. Fiorani, B.R. Webber, Nucl. Phys. B **377**, 445 (1992)
40. E.A. De Wolf, I.M. Dremin, W. Kittel, Phys. Rep. **270**, 1 (1996)
41. MARK I collaboration, J.L. Siegrist et al., Phys. Rev. D **26**, 969 (1982)
42. ARGUS Collaboration, H. Albrecht et al., Z. Phys. C **54**, 13 (1992)
43. JADE Collaboration, W. Bartel et al., Z. Phys. C **20**, 187 (1983)
44. TASSO Collaboration, W. Braunschweig et al., Z. Phys. C **45**, 193 (1989)
45. HRS Collaboration, M. Derrick et al., Phys. Rev. D **34**, 3304 (1986)
46. AMY Collaboration, H.W. Zheng et al., Phys. Rev. D **42**, 737 (1990)
47. ALEPH Collaboration, R. Barate et al., Phys. Rep. **294**, 1 (1998)
48. DELPHI Collaboration, P. Abreu et al., Phys. Lett. B **372**, 172 (1996); B **416**, 233 (1998); Eur. Phys. J. C **6**, 19 (1999)
49. L3 Collaboration, B. Adeva et al., Z. Phys. C **55**, 39 (1992); M. Acciarri et al., Phys. Lett. B **371**, 137 (1996); B **404**, 390 (1997); B **444**, 569 (1998)
50. OPAL Collaboration, G. Alexander et al., Z. Phys. C **72**, 191 (1996); K. Ackerstaff et al., Z. Phys. C **75**, 193 (1997); Eur. Phys. J. C **7**, 369 (1999); G. Abbiendi et al., Eur Phys. J. C **16**, 185 (2000)
51. JADE and OPAL Collaborations, P. Pfeifenschneider et al., Eur. Phys. J. C **17**, 19 (2000); jet multiplicities at small $y_{\rm cut}$ are available from Durham data base at http://durpdg.dur.ac.uk/HEPDATA/REAC, code RED 5019
52. W. Ochs, in New trends in HERA Physics 1999, Lecture Notes in Physics 546, edited by G. Grindhammer, B.A. Kniehl, G. Kramer (Springer, Heidelberg 2000), hep-ph/9911240
53. S. Lupia, W. Ochs, J. Wosiek, Nucl. Phys. B **540**, 405 (1999)
54. TASSO Collaboration, M. Althoff et al., Z. Phys. C **22**, 307 (1984)